Changes of copper location in CuY zeolites induced by preparation methods

J.M. Campos-Martín [a], A. Guerrero-Ruiz [b] and J.L.G. Fierro [a,1]

[a] *Instituto de Catálisis y Petroleoquímica, CSIC, Campus UAM, Cantoblanco, 28049 Madrid, Spain*
[b] *Departamento de Química Inorgánica, UNED, Senda del Rey s/n, 28040 Madrid, Spain*

Received 13 January 1996; accepted 14 June 1996

The location of transition ions in copper- and copper–zinc-loaded Y type zeolites prepared by different procedures has been studied by temperature-programmed reduction, infrared spectroscopy of CO adsorbed on pretreated samples and X-ray photoelectron spectroscopy. Samples outgassed at 673 K showed Cu^+ species due likely to reduction of Cu^{2+} ions under vacuum. Over exchanged CuY zeolites copper species in exchange sites were detected, while an impregnated sample exhibited bands of CO adsorbed on both Cu^{2+} and Cu^+ ions developed at the surface of CuO crystals, and small proportions of Cu^+ ions located in accessible exchange sites S_{II} and $S_{II'}$. Similar findings were observed in Zn- and Cu-exchanged zeolites although the relative proportion of Cu in S_I positions was decreased due to competition between Cu^{2+} and Zn^{2+} ions. Samples reduced in hydrogen at 523 K showed the appearance of Cu^0 species in impregnated samples, whereas Cu^+ dominated in the exchanged counterparts. Reduction at 598 K led to substantial changes in Cu-exchanged samples in water. The proportion of Cu^+ species decreased by reduction to Cu^0 and simultaneously migration to Cu^+ to $S_{II'}$ sites occurred. While Cu^{2+} or Cu^+ were found on outgassed samples, only Cu^0 and intrazeolite Cu^+ were observed after H_2-reduction at 623 K. Changes in copper exposure as a function of sample pretreatments were also revealed by X-ray photoelectron spectroscopy.

Keywords: TPR; FT-IR; XPS; copper location; Y zeolite; ionic exchange; impregnation

1. Introduction

Transition metal ion-exchanged zeolites can be used as catalysts for a wide range of chemical reactions, including dehydrogenation, oxidation, isomerization, cracking of various organic feedstocks, and NO_x elimination. Copper-exchanged Y zeolites have been shown to be highly active and selective catalysts [1–3]. These catalytic properties are mainly explained in terms of both the different oxidation states and the various coordination modes of copper ions, and as a consequence of their location within the zeolite framework [4]. To characterize these catalysts various types of experimental techniques have been employed [4–9]. From these studies, it appeared that in Y zeolites the Cu(II) ions located in the S_I sites were the most difficult species to reduce. Different copper chemical states can be identified and characterized by X-ray photoelectron spectroscopy (XPS) and the modified Auger parameter shifts, such as intrazeolite Cu(II) and Cu(I) zeolites, copper metal clusters or segregated copper metal crystallites [10,11]. The study by infrared spectroscopy of CO is often used as a selective probe for Cu ions because there is a characteristic carbonyl frequency shift depending on the copper oxidation state and its coordination environment [13–15]. This is due to the ability of CO to form complexes in CuY with Cu(I) with a 1 : 1 stoichiometry but not over Cu(II). Moreover, the small size of the CO molecule enables it to diffuse into the sodalite cavities below 373 K. Because Cu^{2+} ions are difficult to monitor by CO-FTIR, complementary techniques such as temperature-programmed reduction (TPR) and XPS must also be employed to provide an accurate assignment of the oxidation state of Cu in zeolites when subjected to various reduction treatments. Less information has been obtained when a second metallic ion is incorporated in Y zeolites together with Cu. Some studies have been carried out over the Zn/NaY system [13,16], but there are limited studies on the effects of coexchange of two metallic ions.

Accordingly, this work was undertaken with the aim to study the effect of the preparation method on the location of copper cations and the changes of its reduction properties by using several techniques, TPR, XPS and FT-IR of adsorbed CO. Moreover, the impact of the simultaneous incorporation of Zn and Cu on the chemical state of copper ions was analyzed.

2. Experimental

2.1. Sample preparation

Samples were prepared starting from a Union Carbide Co. NaY zeolite (LZ-Y52). The reagents were analytical grade $Cu(NO_3)\cdot 3H_2O$ and $Zn(NO_3)\cdot 6H_2O$. The standard conditions for the ion exchange experiments were 30 cm^3 of 0.01 M Cu^{2+} and/or Zn^{2+} solution

---

[1] To whom correspondence should be addressed.

(water or ethanol) on 1 g zeolite for 24 h at room temperature. These samples were repeatedly washed and dried at room temperature overnight. This procedure was repeated three times more. The samples were dried at 383 K for 12 h and then calcined at 673 K for 4 h. For the sample prepared by impregnation, the zeolite was contacted with a solution of copper nitrate in ethanol and the solvent was slowly removed. Subsequently, the impregnate was dried at 383 K for 12 h and then calcined at 673 K for 4 h. For the sake of simplicity, the samples will be referred to hereafter as X^y, where X denotes the added cation (Cu or CuZn) and y the preparation procedure: w, ion exchange in water; e, ion exchange in ethanol; and i, impregnation. The cation content in the final samples was analyzed by atomic absorption spectrometry. From these values the exchange levels summarized in table 1 were determined.

2.2. *Experimental techniques*

Temperature-programmed reduction (TPR) was carried out in a Micromeritics 3000 TPR apparatus by passing a 10% H_2/Ar flow (50 cm^3/min) through the sample. The temperature was increased from 323 to 773 K at a rate of 10 K/min, and the amount of H_2 consumed was determined with a TCD, the effluent gas was passed through a cold trap placed before the TCD in order to remove water from the exit stream.

FT-IR spectra were recorded with a resolution of 4 cm^{-1} in a Nicolet 510 FT-IR spectrophotometer. The wafers (10–12 mg/cm^2) were outgassed under high vacuum at 673 K for 1 h in a glass cell provided with greaseless stopcocks and KBr windows. The outgassed sample was cooled to room temperature and the background spectrum recorded. Subsequently, the sample was exposed to 30 Torr (1 Torr = 133.33 Pa) CO, the gas phase was removed by outgassing at room temperature for 15 min. After recording the spectrum of adsorbed CO, the net spectrum was obtained by subtracting the background spectrum from the latter. To acquire spectra of reduced samples the wafers were treated in the IR cell with a hydrogen flow at 523 or 598 K for 1 h and then the same experimental procedure as above was followed.

XP spectra were acquired with a Fisons Escalab 200R spectrometer equipped with a hemispherical electron analyzer and an Al Kα ($h\nu = 1486.6$ eV, 1 eV = 1.6302×10^{-19} J) 120 W X-ray source. The powder samples were pressed into small aluminum cylinders and then mounted on a sample rod placed in a pretreatment chamber. Prior to being moved into the analysis chamber, the sample was evacuated at 673 K or reduced in situ by H_2 at 473 and 598 K. The pressure in the ion-pumped analysis chamber was maintained below 3×10^{-9} Torr during data acquisition. The intensities of the peaks were estimated by calculating the integral of each peak after smoothing and subtraction of the "S-shaped" background. All binding energies (BE) were referenced to the adventitious C 1s line at 284.9 eV. This reference gave BE values with an accuracy of ±0.2 eV. The Cu_{LMM} Auger peak was also recorded and the modified Auger parameter, $\alpha_{A'}$, calculated by the equation $\alpha_{A'} = h\nu + (\text{KE Cu}_{LMM} - \text{KE Cu } 2p_{3/2})$, where the difference in parentheses represents the difference between the kinetic energy of the Cu_{LMM} Auger electron and the Cu $2p_{3/2}$ photoelectron.

Table 1
Degree of ionic exchange in the different samples obtained by AAS

Sample	Degree of exchange (%)
Cu^i	80 [a]
Cu^w	100
$CuZn^w$	100
Cu^e	91
$CuZn^e$	90

[a] Calculation from Cu content but not in real exchange due to the preparation method.

3. Results and discussion

3.1. *TPR*

The TPR profiles of Cu^i, Cu^w and Cu^e samples are shown in fig. 1. The reduction profile of the sample pre-

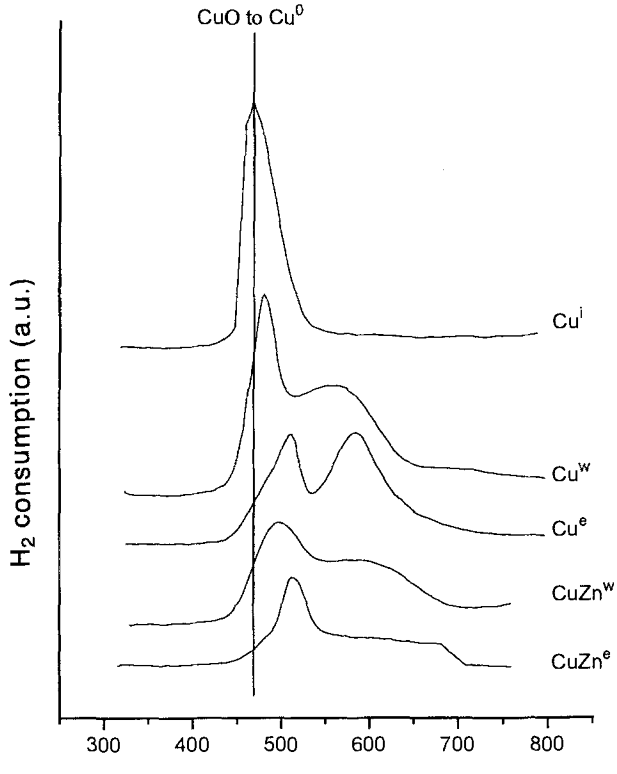

Fig. 1. TPR profiles of CuY zeolite samples prepared by different procedures and TPR profiles of CuZnY zeolite samples in which both copper and zinc were incorporated simultaneously.

pared by impregnation (Cu^i) showed only a peak centred at 467 K, while the exchanged samples exhibited more complex profiles (fig. 1). The sample ion-exchanged in water (Cu^w) had two reduction peaks (fig. 1), the first at 483 K associated with the reduction of Cu^{2+} to Cu$^+$, and the second one at 553 K due to reduction of Cu$^+$ to Cu metal [4,5]. Fig. 1 also displays TPR profiles of CuZnY samples. By the comparison of profiles corresponding to the Cu^w sample and to its CuZn^w counterpart (fig. 1) a delay in Cu reduction temperature due to the presence of Zn can be observed. This effect was similar to that observed in TPR profiles for the CuO/ZnO catalysts in which zinc inhibits copper reduction [17–19]. Samples prepared by ion-exchange in ethanol had different reduction profiles (fig. 1). The Cu^e sample exhibited two well-defined peaks, shifted to higher temperatures by ca. 40 K with respect to the homologous sample prepared in water, Cu^w (fig. 1). The inhibition of reduction by the presence of zinc was again observed in CuZn^e samples, although this effect was less pronounced than in the CuZn^w counterparts. It should be also noted that the exchanged samples displayed a shoulder at low temperature which could be associated with the reduction of a small proportion of CuO to Cu^0, thus indicating the presence of a small amount of copper in the CuO phase, apart from that ion-exchange.

The TPR profiles clearly demonstrated that the preparation method modified the reduction properties of copper. Thus, while impregnated copper was reduced in one step, ionic exchange led to stabilization of Cu$^+$ for which two reduction peaks were distinguished. The solvent employed in the ionic exchange also altered the reduction profiles: samples exchanged in water were reduced at lower temperatures than those exchanged in ethanol. The changes in reduction temperature could be due to the following reasons: (i) the preparation of samples in water facilitated the mobility of copper in the zeolite framework, during the reduction process, which favoured copper ion reduction because this mobility was necessary in the reduction mechanism, as proposed in the bibliography [5]; (ii) using ethanol as solvent, a higher proportion of copper ions were exchanged in sites close to the hexagonal prism, where they are more difficult to reduce [20]. This second effect was confirmed by the FT-IR study of adsorbed CO (see below).

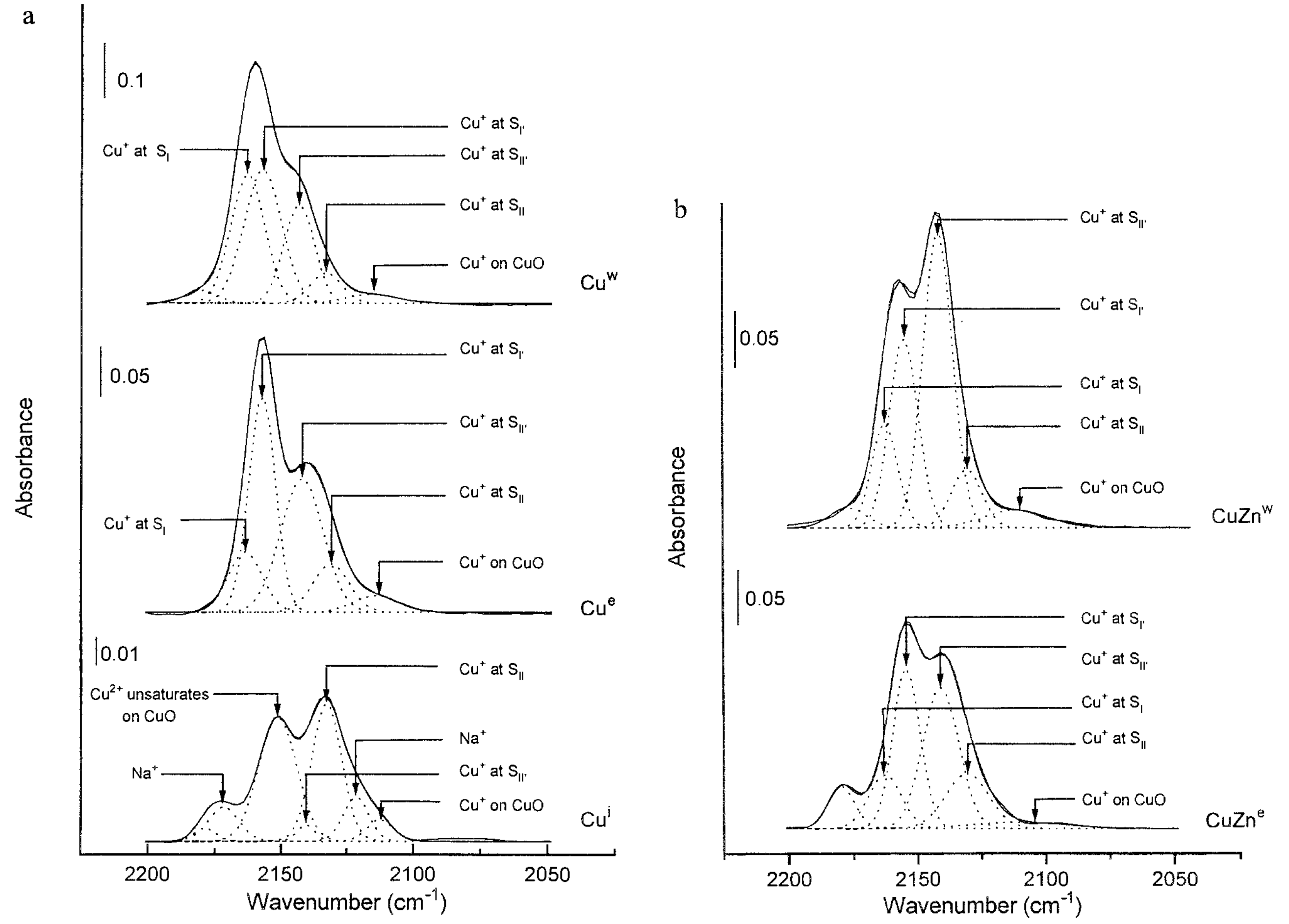

Fig. 2. (a) FT-IR spectra in the CO stretching region of outgassed CuY zeolite samples: (top) Cu^w, (middle) Cu^e, (bottom) Cu^i; (b) FT-IR spectra in the CO stretching region of outgassed CuZnY zeolite samples: (top) CuZn^w, (bottom) CuZn^e.

3.2. FT-IR of adsorbed CO

FT-IR spectra in the CO stretching energy region for different samples are shown in figs. 2–4. These spectra are complex because of the overlapping of several peaks due to CO adsorbed on copper species in different locations. To get better peak differentiation, the experimental curves were fitted to a sum of Gaussian distributions. This fitting was achieved by minimizing the χ^2 value using the Levenberg–Marquart algorithm [21]. Accordingly, several CO species adsorbed on copper could be identified corresponding to: (i) Cu^+ in CuO surface extra framework of zeolite, 2115 cm^{-1} [22]; (ii) Cu^+ in exchange sites, S_{II} and $S_{II'}$, 2132 and 2144 cm^{-1}, respectively [15]. When we tried to fit the peak attributed to CO adsorbed on Cu^+ at S_I and $S_{I'}$, at 2160 cm^{-1} as already done in the literature, the center of this band fluctuated, depending on the preparation procedure or sample pretreatment. This fact suggested that this band at 2160 cm^{-1} might well involve two different components, whose relative intensities would affect the envelope centre. Consistently with this a fitting, involving two peaks, for such a band was made which may account for two types of exchange sites. The best results were obtained by assigning the wavenumber of 2157 cm^{-1} to CO adsorbed on Cu^+ at $S_{I'}$ and 2164 cm^{-1} to CO adsorbed on Cu^+ at S_I. This assignment of the two very close bands was made considering that the more distorted species Cu^+–CO at S_I corresponded to the higher frequency.

Samples treated under vacuum at 673 K show Cu^+ species in all cases (fig. 2), probably due to reduction of Cu^{2+} to Cu^+ under vacuum. In the Cu^i sample, the presence of copper oxide was evident, as revealed by the appearance of bands corresponding to CO on unsaturated Cu^{2+} sites on CuO (2150 cm^{-1}) [23] and CO–Cu^+ on CuO (2112 cm^{-1}) [12]. Furthermore, a small proportion of Cu^+ was detected at more accessible exchange sites S_{II} and $S_{II'}$ (fig. 2), but with a lower intensity with respect to Cu^w and Cu^e samples. In these latter samples, the signal was mainly due to exchanged copper and only a low intense peak of Cu^+ on CuO (2114 cm^{-1}) appeared (fig. 2).

The exchange of a second cation (Zn^{2+}) led to an increase in the intensity of the band of CO adsorbed on Cu^+ at site $S_{II'}$ with respect to S_{II} and a decrease of that of CO adsorbed at site S_I with respect to $S_{I'}$ could be observed (fig. 2). This effect seems to be less marked in the $CuZn^e$ sample. This might be due to the fact that, in spite of the preferential location of copper cations in sites close to the hexagonal prisms on dehydrated zeolites, a higher proportion of copper in sites near supercages is

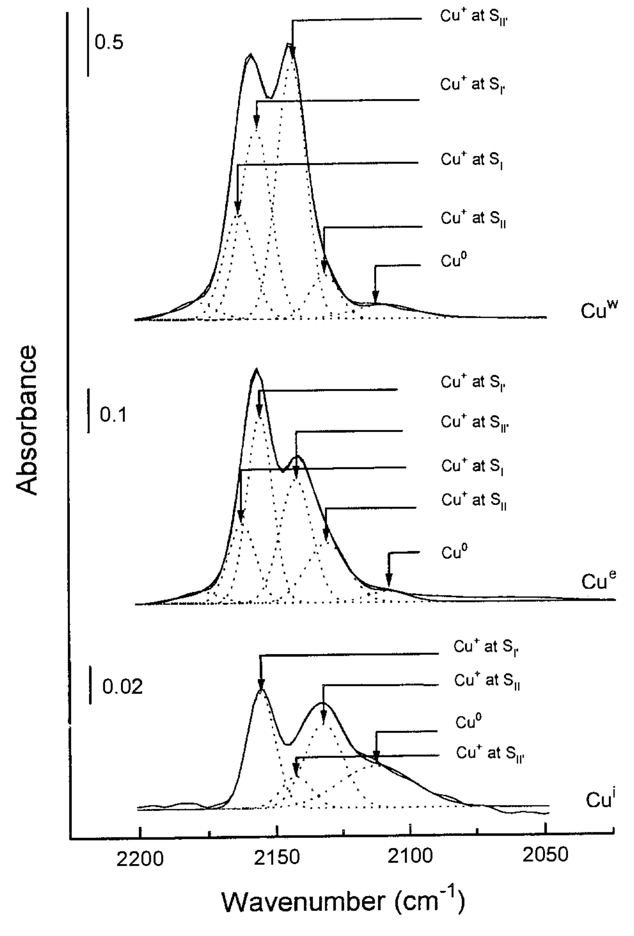

Fig. 3. FT-IR spectra in the CO stretching region of H_2 reduced CuY zeolite samples at 523 K: (top) Cu^w, (middle) Cu^e, (bottom) Cu^i.

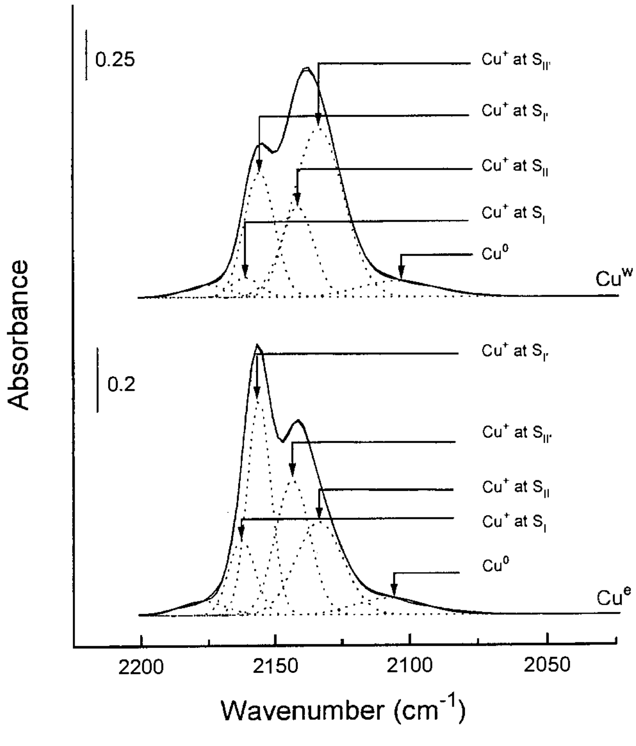

Fig. 4. FT-IR spectra in the CO stretching region of H_2 reduced CuY zeolite samples at 598 K: (top) Cu^w, (bottom) Cu^e.

formed very likely from the competition between copper and zinc for S_I sites in the binary $CuZn^y$ samples.

FT-IR spectra of samples reduced at 523 K are shown in fig. 3. In all samples the peak of CO adsorbed on Cu^+ on CuO disappeared, and simultaneously a low intense peak of CO on Cu^0 (2108 cm^{-1}) was detected. The sample prepared by impregnation displayed a very weak band (fig. 3), with a high contribution of CO–Cu^0. Neither Cu^{2+} on CuO nor Cu^+ on CuO were detected, although a weak band of exchanged copper was also observed. Exchanged samples displayed an increase in the band with respect to their outgassed counterparts. This was in agreement with TPR profiles which indicate that the transition of Cu^{2+} to Cu^+ had already occurred, with the CO complex on Cu^+ more favoured. It should be noted that the Cu^e sample displays a higher proportion of copper exchanged in sites close to the hexagonal prism than Cu^w (fig. 3). This finding can be explained on the basis that copper ions in presence of water tend to be located in more external sites of the Y zeolite [24]. Accordingly, when water is used as a solvent large proportions of copper were exchanged in the sites close to supercages, while exchange in sites S_I and $S_{I'}$ could be favoured in ethanol.

After reduction at 598 K some changes in FT-IR spectra of adsorbed CO were observed (fig. 4). While Cu^e did not exhibit important changes with respect to its counterpart reduced at 523 K (figs. 3 and 4), probably because at these temperatures, as shown by TPR experiments, copper was not reduced to Cu^0, for the sample Cu^w an important decrease in the intensity of the bands with respect to that reduced at 523 K (figs. 3 and 4) was observed. This effect could be attributed to the partial reduction of Cu^+ to Cu^0, as TPR experiments for this sample showed. A further observation was the relative increase of the CO–Cu^+ band at the S_{II} site, which was indicative of a migration of copper species to sites in or near to supercages, but not to a reduction of copper in internal sites since this would require higher temperatures [15]. The migration of copper after pretreatments was confirmed by the XPS Cu/Si atomic ratios (see below).

3.3. XPS

The binding energy of the Cu $2p_{3/2}$ core level and the Auger parameter of samples subjected to several pretreatments in situ – outgassing at 673 K, or reduction in hydrogen at 473 or 623 K – are compiled in table 2. By combining binding energy and Auger parameter over the Wagner plot the different chemical states of copper could be identified [11]. These copper species are summarized in table 2. A change in the copper species with the pretreatments and preparation procedure was evi-

Table 2
Binding energy (eV) of core electrons, modified Auger parameter, copper species identified by XPS and Cu/Si atomic ratios on samples subjected to pretreatments in situ

Sample	Treatment	Cu $2p_{3/2}$	$\alpha_{Cu'}$	Cu/Si at	Cu species
Cu^i	vac, 673 K	932.7(40) 934.1(60)	1849.0 1851.3	0.118	Cu^+ external Cu^{2+} external
	H_2, 473 K	932.6(88)	1851.4	0.073	Cu^0 external
	H_2, 623 K	932.6	1851.5	0.078	Cu^0 external
Cu^w	vac, 673 K	933.2(76) 935.5(24)	1845.9 1851.7	0.056	Cu^+ exchanged Cu^{2+} exchanged
	H_2, 473 K	933.1(85) 935.5(15)	1845.6 1851.4	0.073	Cu^+ exchanged Cu^{2+} exchanged
	H_2, 623 K	933.0 933.0 934.2	1845.6 1850.3 1854.6	0.132	Cu^+ exchanged Cu^0 external Cu^0 supercage
Cu^e	vac, 673 K	932.9(64) 936.0(36)	1846.0 1851.3	0.038	Cu^+ exchanged Cu^{2+} exchanged
	H_2, 473 K	933.0(78) 936.2(22)	1846.2 1851.0	0.050	Cu^+ exchanged Cu^{2+} exchanged
	H_2, 623 K	933.0 933.0 934.2	1845.9 1851.4 1854.1	0.093	Cu^+ exchanged Cu^0 external Cu^0 supercage

dent. The outgassed sample prepared by impregnation showed only external copper, Cu^{2+} or Cu^+, the reduced species probably formed during outgassing at 673 K. After reduction at 473 K or at 623 K only external metallic copper was observed. Exchanged samples showed intrazeolite Cu^{2+} and Cu^+ after outgassing, Cu^+ species probably formed under outgassing. Samples reduced at 473 K exhibited the same species, only Cu^+ displayed a higher proportion than in its outgassed counterpart. However, a higher proportion of Cu^{2+} species was observed in Cu^e then in Cu^w. This observation could be explained by the more difficult reduction of this sample, as revealed by TPR. After reduction at 623 K, Cu^{2+} species were not detected, only intrazeolite Cu^+ and Cu^0 external zeolite framework and Cu^0 clusters in the supercages were observed. Due to the difficulty to obtain quantitative values of Cu_{LMM} peak intensities, the relative proportion of each species is not reported.

The relative surface exposure of copper, as measured by Cu/Si ratios, is given in table 2. This ratio depended on the preparation method. For the sample prepared by impregnation, this proportion decreased with the reduction treatment at 473 and 623 K, probably due to sinterization of copper particles on the external surface of the zeolite. For the exchanged samples, an increase of the Cu/Si ratio was observed. This result could be explained as due to a limitation of the XPS technique, even though X-rays penetrate a few microns into the solid, Cu $2p_{3/2}$ photoelectrons could only come from the more accessible zones of the zeolite. As a consequence, an increase in the Cu/Si ratio could be attributed to migration of copper species from internal positions to the external zeolite surface when the reduction temperature was increased. This observation agrees with the appearance of metallic copper at the external surface and Cu^0 clusters in supercages as identified in Cu^w and Cu^e samples reduced at 623 K by XPS, and the FT-IR of adsorbed CO which showed a higher proportion of copper in external exchange positions after reduction at 598 K.

4. Conclusions

The preparation method modified the reduction properties of copper. Thus, while impregnated copper was reduced in one step, two reduction peaks were distinguished in the exchanged samples. The solvent employed for the ionic exchange also altered the reduction profiles: samples exchanged in water were reduced at lower temperatures than those exchanged in ethanol. Inhibition of copper reduction by the presence of zinc is observed in CuZnY samples, similar to that observed in TPR profiles for the CuO/ZnO catalysts.

During the study of FT-IR spectra in the CO stretching energy region, two experimental bands were assigned by fitting the experimental bands to Gaussian distributions: the wavenumber of 2157 cm^{-1} to CO adsorbed on Cu^+ at $S_{I'}$, and 2164 cm^{-1} to CO adsorbed on Cu^+ at S_I. The copper location was modified by the preparation procedure: while exchanged CuY zeolites showed copper species in exchange sites, the impregnated sample exhibited bands of CO adsorbed on both Cu^{2+} and Cu^+ ions developed at the surface of CuO crystals, and small proportions of Cu^+ ions placed in accessible exchange sites S_{II} and $S_{II'}$. The exchange of a second cation (Zn^{2+}) had no significative effect, although the relative proportion of Cu in S_I locations decreased due to competition between Cu^{2+} and Zn^{2+} ions.

Copper oxidation state and its location was affected by pretreatments with hydrogen. Samples reduced at 523 K showed the appearance of Cu^0 species in impregnated samples, whereas Cu^+ dominated in exchanged counterparts, on the other hand reduction at 598 K led to substantial changes in Cu exchanged samples in water, as the decrease in the proportion of Cu^+ species by reduction to Cu^0 and simultaneously migration of Cu^+ to external sites. Only Cu^0 and intrazeolite Cu^+ were observed after H_2-reduction at 623 K.

Acknowledgement

The financial support of this work by Comisión Interministerial de Ciencia y Tecnología (projects MAT91-0494 and AMB93-1426-CE) is gratefully acknowledged. JMCM thanks the Ministerio de Educacion y Ciencia for a fellowship grant.

References

[1] V.K. Kaushik and M. Ravindranathan, Zeolites 12 (1992) 415.
[2] M. Nargama, S. Contarini and L. Kevan, J. Catal. 94 (1985) 370.
[3] I.E. Maxwell, R.S. Downing and S.A.J. van Langen, J. Catal. 61 (1980) 485.
[4] H. Matsumoto and S. Tanabe, J. Phys. Chem. 94 (1990) 4207.
[5] P.A. Jacobs, M. Tielen, J.-P. Linart, J.B. Uytterhoeven and H. Beyer, J. Chem. Soc. Faraday Trans. 72 (1976) 2793.
[6] J.C. Conesa and J. Soria, J. Phys. Chem. 82 (1978) 1575.
[7] I.E. Maxwell, J.J. de Boer and R.S. Downing, J. Catal. 61 (1980) 493.
[8] S.B. Liu, T.S. Lin, T.C. Yang, T.H. Chen, E.C. Hong and R. Ryoo, J. Phys. Chem. 99 (1995) 8277.
[9] R.A. Schoonheydt, Catal. Rev. Sci. Eng. 35 (1993) 129.
[10] I. Jirka and V. Bosacek, Zeolites 11 (1991) 77.
[11] G. Moretti, Zeolites 14 (1994) 469.
[12] C.L. Angell and P.C. Schaffer, J. Phys. Chem. 70 (1966) 1413.
[13] Y.Y. Huang, J. Catal. 61 (1980) 461.
[14] C. Marquez-Alvarez, G.S. McDowgall, A. Guerrero-Ruiz and I. Rodriguez-Ramos, Appl. Surf. Sci. 78 (1994) 477.
[15] J. Howard and J.M. Nicol, Zeolites 8 (1988) 142.
[16] K. Otsuka, J. Mamda and A. Morikawa, J. Chem. Soc. Faraday Trans. I 77 (1981) 2429.
[17] A.L. Boyce, S.R. Graville, P.A. Sermon and M.S.W. Wong, React. Kinet. Catal. Lett. 44 (1991) 1.
[18] M.S.W. Wong, P.A. Sermon and K. Grant, Catal. Lett. 4 (1990) 15.

[19] J.M. Campos-Martín, A. Guerrero-Ruiz and J.L.G Fierro, J. Catal. 156 (1995) 208.

[20] C. Naccache and Y. Ben Taarit, J. Catal. 22 (1978) 171.

[21] H.W. Press, B.P. Flamery, S.A. Teuklasky and W.T. Vetterling, in: *Numerical Recipes in C, The Art of Science Computing* (Cambridge University Press, New York, 1988).

[22] A.A. Davidov and A.A. Budneva, React. Kinet. Catal. Lett. 25 (1984) 121.

[23] G. Busca, J. Mol. Catal. 43 (1987) 225.

[24] G. Maccabe and Y. Ben Taarit, Chem. Phys. Lett. 11 (1971) 11.